



## STUDY OF MECHANICAL PROPERTIES OF COMPOSITE WITH SILICONE MATRIX TO MIMETIZATE BIOLOGICAL TISSUE

Marcio Gabriel Moura Netto, Luiz Carlos da Silva Nunes<sup>(1)</sup>

(1) Department of Mechanical Engineering (PGMEC), Universidade Federal Fluminense, Brazil

<https://doi.org/10.21452/bccm4.2018.13.02>

### Abstract

It is of scientific interest to know the mechanical properties of biological materials so they can be reproduced in synthetic materials, since the study in living tissues is often arduous. Silicone is one of the synthetic materials most used to mimic the properties of biological tissues. The present study has as objective to verify the relationship between the orientation of the fibers arranged in a silicone matrix composite. A relationship was found between the orientation of the fibers and the mechanical properties of the material, since when the force is applied in the same direction of the fibers, there is an increase in the mechanical strength and a decrease in the elasticity of the material. It was possible to observe that the mechanical behavior of the material was similar to that found in the literature, being possible to conclude that the work was successful in its objective.

**Keywords:** Silicone, composites, mechanical properties

### 1. INTRODUCTION

It is of scientific interest to know the mechanical properties of biological materials in such a way that they can be reproduced in synthetic materials, since the study in living tissues is arduous and often conflicts with ethical and legal principles. With the help of the principles of mechanical engineering it is possible to understand the normal functions of organisms, to predict changes and to propose artificial methods of interventions [1].

Among the synthetic materials most used to mimic the properties of biological tissues there is the silicone [2,3]. Both living and synthetic tissues are referred to as hyperelastic materials or elastic materials of Green, and the stress components are obtained through the deformation energy of the body [4].

The mechanical behavior of real materials can be described through constitutive equations [5-10]. In the comparison between the main mathematical models that describe hyperelastic materials for the characterization of different biological tissues, it was possible to affirm that synthetic silicone rubber fabrics are better characterized by these equations than the living tissues [11].

The present work consists in the mechanical characterization of a sample of silicone matrix, in order to predict the behavior of living tissues. For this purpose, the deformation data obtained through the digital image correlation technique during the tensile tests are used in the constitutive equations of hyperelastic materials.

## 2. OBJECTIVE

### 2.1 General Objective

Verify the relationship between the orientation of the fibers arranged in a silicone matrix composite.

### 2.2 Specific Objective

To manufacture polymeric composite samples of silicone matrix with cotton fibers in different orientations;

Testing the specimens produced in a traction machine;

Obtain the experimental behavior of these materials from tensile tests;

Apply the technique of correlation of digital images for acquisition of displacement field;

Apply mathematical model based on the concept of strain energy, to determine the mechanical properties of these composites;

## 3. MATERIALS AND METHODS

For this work were used bi-component vulcanized silicone rubber RTV-2 model 4-150 RTV of the brand Moldflex and fibrous cotton fabric. From the fabrication of the composite material, samples were obtained with the same dimensions and with fibers oriented at 0°, 45° and 90° and also produced test pieces consisting only of silicone.

Initially, fiber-free silicone rubber was manufactured and a mold with dimensions 220 mm long, 160 mm wide and 3.8 mm high was used to contain the liquid silicone to be used in the experiment. To facilitate removal of the final material, traditional model of the Grand Prix molding wax was used on a glass plate containing the mold.

The production of the silicone rubber was carried out according to the manufacturer's instructions. For complete cure the T-40 catalyst was added to this material in a proportion equivalent to 3% of the mass of silicone used. From the mold volume and the silicone density provided by the manufacturer, it was possible to know the total mass of silicone and catalyst to be produced. This mixture was poured onto level glass plate evenly spreading through the mold. Figure 1 shows materials and utensils used and the polymer being manufactured.



**Figure 1: Materials used (left) and fabricated silicone rubber (right).**

Subsequently, composite materials consisting of layers of silicone rubber interspersed with cotton fibers were fabricated. As well as for the manufacture of pure silicone, a glass plate

previously treated with a release agent, height regulating support and level ruler was used, but there was no need to use a mold, since the rubber was applied with the help of a roll of foam. Figure 2 shows the manufacturing process that resulted in composites formed by four silicone matrix slides and three cotton fibers slides.



**Figure 2: Manufacturing process of composite materials.**

After the curing process, the excess silicone was removed and the fabricated composites were sectioned in the shape of specimens.

From each material were obtained specimens of same dimensions, and for the composites there was differentiation as to the orientation of the fibers. Afterwards, these materials were randomly painted with spray of black paint, according to figure 3 and tested in a traction machine.

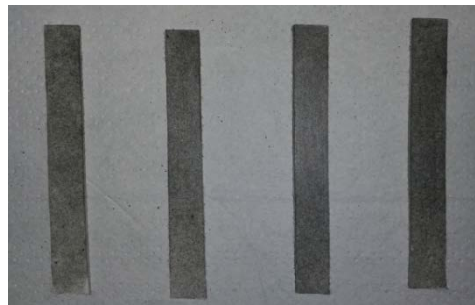


**Figure 3: Specimens.**

In order to obtain the mechanical properties of the materials produced, tensile tests were carried out. Figure 4 shows the apparatus used, which has in its center the specimens connected to the traction machine through two jaws that hold the lower and upper ends of this specimens. Between the upper claw and the traction machine there is a 100kgf load cell, responsible for measuring the force applied throughout the process. The high-resolution Sony XCD-SX900 camera associated with the Digital Image Correlation (DIC) system positioned perpendicular to the samples is responsible for capturing images of the specimen during the test. The obtained data were processed, thus obtaining the fields of material displacement.

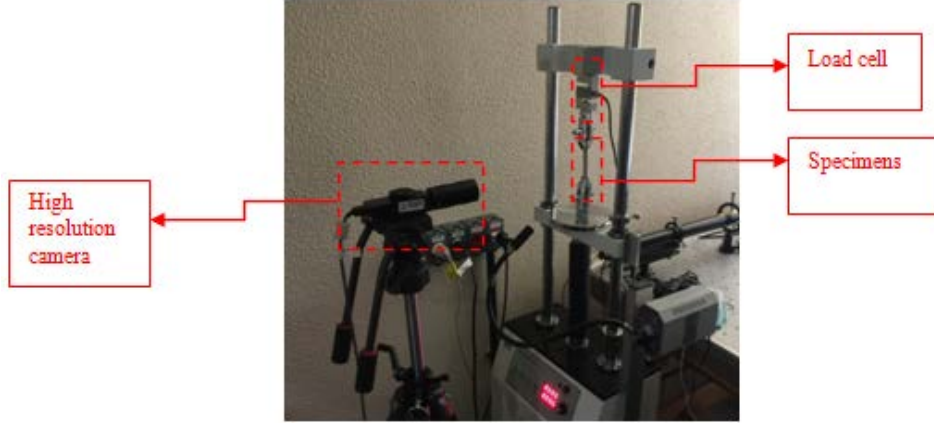


Figure 4: Test Apparatus.

#### 4. MATHEMATICAL METHOD

The developed model considers that the silicone rubber, when submitted to the uniaxial traction, presents behavior similar to that of incompressible hyperelastic materials [11].

Figure 5 is the schematic representation of an infinitesimal element in the reference configuration, with coordinates  $\mathbf{X} = (X_1, X_2, X_3)$  while  $\mathbf{a}_0$  is the unit vector that defines the direction of the fiber in that configuration.

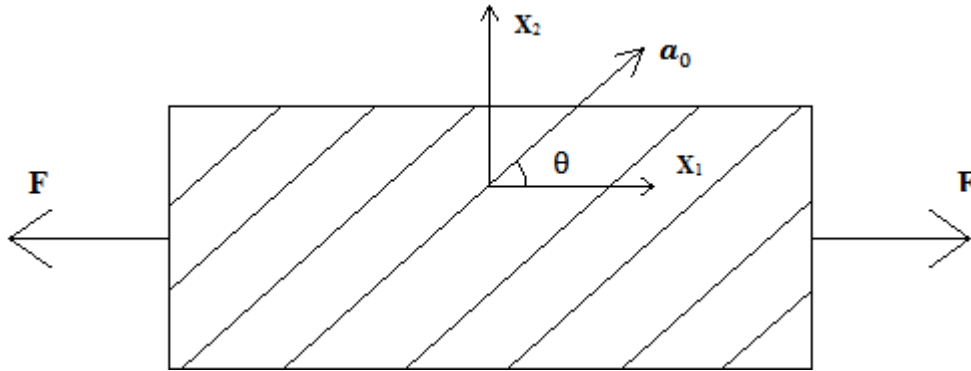


Figure 5: Infinitesimal element.

From the stretching ( $\lambda$ ), which is the scalar value responsible for relating the configuration change of the body, it is possible to obtain the second-order tensor ( $\mathbf{F}$ ) called the strain gradient.

$$\mathbf{F} = \frac{\partial \mathbf{x}}{\partial \mathbf{X}} = \begin{bmatrix} \lambda_1 & 0 & 0 \\ 0 & \lambda_2 & 0 \\ 0 & 0 & \lambda_3 \end{bmatrix} \quad (1)$$

With this result the Cauchy-Green deformation tensor on the left is calculated,  $\mathbf{B} = \mathbf{F}\mathbf{F}^T$ , and the invariants  $I_1 = \text{tr}(\mathbf{B})$ ,  $I_2 = \frac{1}{2}[(\text{tr}\mathbf{B})^2 - \text{tr}\mathbf{B}^2]$ ,  $I_3 = \det\mathbf{B}$ , in addition to the pseudo-invariant  $I_4 = \mathbf{a} \cdot \mathbf{a} = \mathbf{a}_0$ .

For the study of incompressible composites composed of non-linear isotropic matrix and reinforced by unidirectional fibers, one of the most aborted mathematical models in the literature [12] is the so-called standard reinforcement model, in which the strain energy is given by:

$$\Psi = \frac{\mu}{2} [I - 3 + \gamma(I - 2)^2] \quad (2)$$

Let  $\mu$  be the shear modulus of the composite matrix, while  $\gamma$  is the constant that provides a measure of the reinforcing force in the direction of the fiber.

The constitutive equation of the Cauchy stress for transversely isotropic incompressible hyperelastic materials subjected to uniaxial traction is given, according to [13], by:

$$\boldsymbol{\sigma} = -p\mathbf{I} + 2\frac{\partial\Psi}{\partial I_1}\mathbf{B} - 2\frac{\partial\Psi}{\partial I_2}\mathbf{B}^{-1} + 2\frac{\partial\Psi}{\partial I_4}\mathbf{a} \otimes \mathbf{a} \quad (3)$$

In which  $p$  is the arbitrary hydrostatic pressure resulting from the incompressibility hypothesis. The components of this Tensor are given below.

$$\begin{aligned} \sigma_{11} &= -p + \mu\lambda_1^2 + 2\mu\gamma(\lambda_1^2\cos^2\theta + \lambda_2^2\sin^2\theta - 1)\lambda_1^2\cos^2\theta \\ \sigma_{22} &= -p + \mu\lambda_2^2 + 2\mu\gamma(\lambda_1^2\cos^2\theta + \lambda_2^2\sin^2\theta - 1)\lambda_2^2\sin^2\theta \\ \sigma_{33} &= -p + \mu\lambda_3^2 \end{aligned} \quad (4)$$

If the load is uniaxial, then  $\sigma_{22}=\sigma_{33}$ , and the material is incompressible ( $\lambda_1\lambda_2\lambda_3 = 1$ ) it is possible to determine the value of  $\sigma_{11}$  when the test is performed in the fiber direction, according to equation (5).

$$\sigma_{11} = -\frac{\mu}{\lambda} + \mu\lambda_1^2 + 2\mu\gamma\lambda_1^4 - 2\mu\gamma\lambda_1^2 \quad (5)$$

For composites with fibers oriented at 45 ° and 90 °, it is assumed that  $\lambda_2 = \alpha\lambda_1$  and  $\lambda_3 = \beta\lambda_1$ , respectively. So, in the case of fibers oriented at 45 °, the stress  $\sigma_{11}$  is given by equation (6).

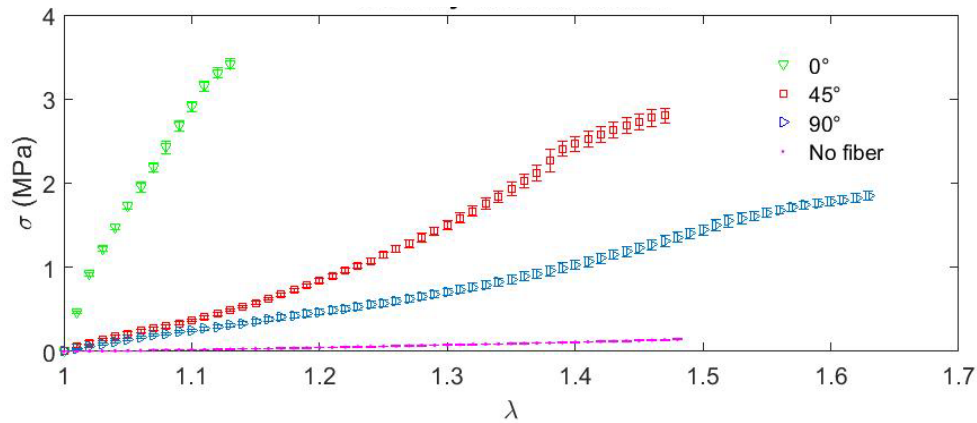
$$\sigma_{11} = \mu\lambda_1^2(\alpha^2 + 2\gamma\alpha^2\lambda_1^2 + 2\gamma\alpha^4\lambda_1^2 - 2\gamma\alpha^2 + 1 + 2\gamma\lambda_1^2 + 2\gamma\alpha^2\lambda_1^2 - 2\gamma) \quad (6)$$

For the case of fibers oriented at 90 °, the stress  $\sigma_{11}$  is given by equation (7)

$$\sigma_{11} = \mu\lambda_1^2(\beta^2 + 2\gamma\beta^4\lambda_1^2 - 2\gamma\beta^2 + 1) \quad (7)$$

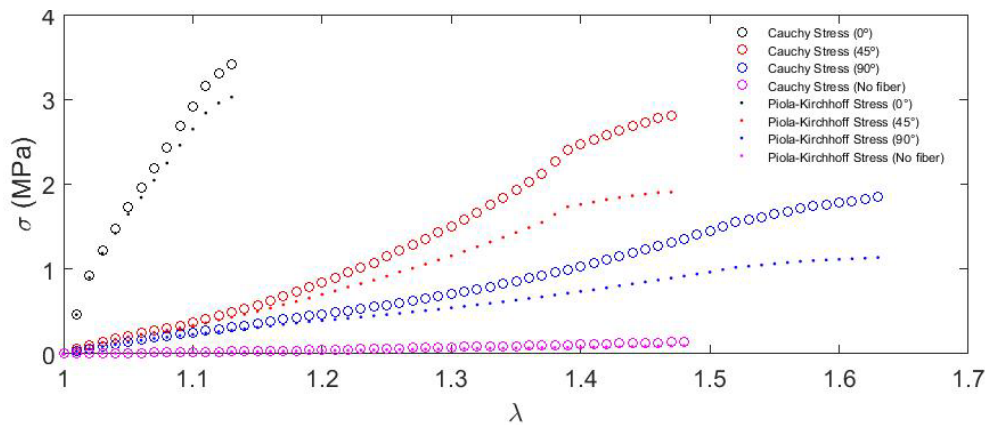
## 5. RESULTS AND DISCUSSIONS

Figure 6 shows the relationship between the stretches undergone by the fiber test specimens in different orientations and the real or applied Cauchy stress. It is possible to notice that the smaller the angle between the direction of the fiber and the direction of application of the force, the greater the tension generated during deformation of the



**Figure 6: Cauchy stress curve.**

Figure 7 shows a comparison between the Cauchy voltages and the Piola-Kirchhoff engineering voltages (or nominal voltages). It is possible to observe that for small deformations there is a coincidence between the applied stresses, however, as expected, for large deformations the real tensions are greater than the Piola-Kirchhoff tensions, since, the real tension considers the decrease of the cross section of the body of evidence.



**Figure 7: Real and engineering stress versus stretching.**

In analyzing Figures 6 and 7 it is possible to notice that the results are in agreement with those found by other authors [14,15], being visible the change of the behavior initially linear to non-linear, when the specimens are submitted to great deformation and increasing the strength of the material according to the arrangement of the fibers, as shown in Table 1.

**Table 1: relation on the resistance of materials.**

Fiber angle	Tensile strength
0°	3,42
45°	2,8
90°	1,85
No fiber	0,14

Figure 8 shows the comparison between the results obtained experimentally and those obtained through the application of the standard reinforcement model, while the correlation coefficient ( $R^2$ ) between these results and the values of the constants of the materials are presented in table 2. It is possible to perceive that the theoretical model adopted presents a good correlation with the experimental results, but this model does not consider changes in the structure of the material, which justifies the lack of correlation with the final phase of the experiment, at which moment the rupture is initiated of the reinforcing fibers.

The values of  $\gamma$  found are in agreement with the expected one, since this constant is related to the degree of reinforcement that the fiber grants to the material. The value of  $\mu$  is the same for all materials, since this constant belongs to the matrix [12].

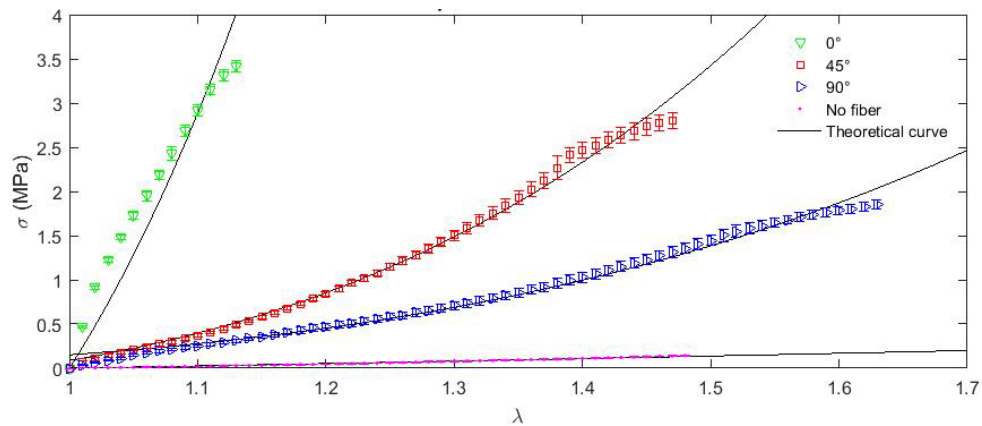


**Figure 8: Comparative chart between experimental and theoretical results.**

**Table 2: Material constants and correlation coefficients.**

Fiber angle	Values		
	$\mu$	$\gamma$	$R^2$
0°	0,08699	64,65	0,8891
45°	0,08699	6,59	0,9937
90°	0,08699	2,37	0,9889
No fiber	0,08699	-	0,9861

## 6. CONCLUSION

It was possible to observe that the mechanical behavior of the material was similar to that found in the literature. In addition, its strength is directly related to the orientation of the fibers constituting the composite material.

The equations of the mathematical model used generated similar theoretical results to the experimental results and the values of the constants found are within the expected, being the value of  $\gamma$  increasing according to the rigidity of the composite. Therefore, it was possible to conclude that the work was successful in its objective.

## **8. ACKNOWLEDGEMENTS**

The financial support of Rio de Janeiro State Funding (FAPERJ), and Research and Teaching National Council, CNPq, are gratefully and acknowledged.

## **9. REFERENCES**

- [1] FUNG, Yuan-cheng. Biomechanics: mechanical properties of living tissues. Springer Science & Business Media, 2013.
- [2] SAAGER, Rolf B. et al. Multilayer silicone phantoms for the evaluation of quantitative optical techniques in skin imaging. In: Design and Performance Validation of Phantoms Used in Conjunction with Optical Measurement of Tissue II. International Society for Optics and Photonics, p. 756706, 2010.
- [3] SPARKS, Jessica L. et al. Use of silicone materials to simulate tissue biomechanics as related to deep tissue injury. *Advances in skin & wound care*, v. 28, n. 2, p. 59-68, 2015.
- [4] KULKARNI, S. G. et al. A transversely isotropic visco-hyperelastic constitutive model for soft tissues. *Mathematics and Mechanics of Solids*, v. 21, n. 6, p. 747-770, 2016.
- [5] SASSO, M. et al. Characterization of hyperelastic rubber-like materials by biaxial and uniaxial stretching tests based on optical methods. *Polymer Testing*, v. 27, n. 8, p. 995-1004, 2008.
- [6] MARCKMANN, Gilles; VERRON, Erwan. Comparison of hyperelastic models for rubber-like materials. *Rubber chemistry and technology*, v. 79, n. 5, p. 835-858, 2006.
- [7] DIANI, Julie et al. Directional model for isotropic and anisotropic hyperelastic rubber-like materials. *Mechanics of Materials*, v. 36, n. 4, p. 313-321, 2004.
- [8] HORGAN, Cornelius O.; SMAYDA, Michael G. The importance of the second strain invariant in the constitutive modeling of elastomers and soft biomaterials. *Mechanics of Materials*, v. 51, p. 43-52, 2012.
- [9] HOLZAPFEL, Gerhard A.; GASSER, Thomas C.; OGDEN, Ray W. A new constitutive framework for arterial wall mechanics and a comparative study of material models. *Journal of elasticity and the physical science of solids*, v. 61, n. 1-3, p. 1-48, 2000.
- [10] DESYATOVA, Anastasia; MACTAGGART, Jason; KAMENSKIY, Alexey. Constitutive modeling of human femoropopliteal artery biaxial stiffening due to aging and diabetes. *Acta biomaterialia*, v. 64, p. 50-58, 2017.
- [11] MARTINS, P. A. L. S.; NATAL JORGE, R. M.; FERREIRA, A. J. M. A comparative study of several material models for prediction of hyperelastic properties: Application to silicone-rubber and soft tissues. *Strain*, v. 42, n. 3, p. 135-147, 2006.
- [12] MERODIO, J.; OGDEN, R. W. Mechanical response of fiber-reinforced incompressible non-linearly elastic solids. *International Journal of Non-Linear Mechanics*, v. 40, n. 2-3, p. 213-227, 2005.
- [13] Holzapfel, G. A., *Nonlinear Solid Mechanics*, John Wiley & Sons LTD, pp. 205-304, 2000.
- [14] KIM, Beomkeun et al. A comparison among Neo-Hookean model, Mooney-Rivlin model, and Ogden model for chloroprene rubber. *International Journal of Precision Engineering and Manufacturing*, v. 13, n. 5, p. 759-764, 2012.
- [15] NERURKAR, Nandan L.; ELLIOTT, Dawn M.; MAUCK, Robert L. Mechanics of oriented electrospun nanofibrous scaffolds for annulus fibrosus tissue engineering. *Journal of orthopaedic research*, v. 25, n. 8, p. 1018-1028, 2007.